Solution-processed bulk heterojunction organic solar cells based on an oligothiophene derivative

Bin Yin,[1,a)] Liying Yang,[1] Yongsheng Liu,[2] Yongsheng Chen,[2] Qingjin Qi,[1] Fengling Zhang,[1,3] and Shougen Yin[1,b)]

[1]*Key Laboratory of Display Materials and Photoelectric Devices, Ministry of Education, Institute of Material Physics, and Tianjin Key Laboratory for Photoelectric Materials and Devices, Tianjin University of Technology, Tianjin 300384, People's Republic of China*
[2]*Key Laboratory for Functional Polymer Materials and Center for Nanoscale Science and Technology, Institute of Polymer Chemistry, College of Chemistry, Nankai University, Tianjin 300071, People's Republic of China*
[3]*Department of Physics, Chemistry, and Biology (IFM), Biomolecular and Organic Electronics, Center of Organic Electronics, Linköping University, SE-58183 Linköping, Sweden*

Organic bulk heterojunction (BHJ) solar cells based on a dicyanovinyl-substituted oligothiophene as a donor and [6,6]-phenyl C61 butyric acid methyl ester (PCBM) as an acceptor were fabricated and characterized. The oligothiophene derivative can absorb long wavelength photons of the solar radiation, which makes the solar cells with an optimized weight ratio of 1:1.4 have a decent short-circuit current density (12.4 mA/cm^2) and open-circuit voltage (0.88 V) under AM 1.5G illumination with an intensity of 100 mW/cm^2. A power conversion efficiency (PCE) of 3.7% is achieved, which is among the best PCEs of solution processed small molecule BHJ solar cells. © *2010 American Institute of Physics*. [doi:10.1063/1.3460911]

Bulk heterojunction (BHJ) solar cells based on conjugated polymer/fullerene systems are evolving into a promising phase for low-cost photovoltaic applications due to solution processing, light weight, and large scale flexible devices.[1,2] The power conversion efficiency (PCE) of the devices based on these materials are predicted to reach 15% by modeling.[3] At present, the solar cells based on poly(3-hexyl thiophene) (P3HT):[6,6]-phenyl C61 butyric acid methyl ester (PCBM) attract a great deal of attention and have demonstrated efficiencies as high as 5%–6%.[4] In recent years, solution processable BHJ organic solar cells based on conjugated small molecules and fullerenes have been extensively investigated.[5–11] Solution processable small molecules have numerous merits, such as, high chemical stability, high carrier mobility, well defined structures, easy synthesis and purification, intrinsically monodisperse, and few deep electron traps in solid films.[12–14] Oligothiophenes possess the above advantages, which makes them promising donors for solution processed BHJ solar cells when blend them with PCBM. PCE up to 2.3% and 3.0% were demonstrated using an oligothiophene with a dialkylated diketopyrrolopyrrole chromophore as a donor and soluble fullerenes PCBM or [6,6]-phenyl C71 butyric acid methyl ester as an acceptor, respectively.[10,11] The best performance of solution processed small molecule solar cells with a PCE of 4.4% was reported by Nguyen *et al.*[15]

In this letter, the donor used for the BHJ solar cells was an oligothiophene derivative 5,5′′′′′′-bi(dicyanovinyl)-3,3′,3′′,3′′′,3′′′′,3′′′′′-sexioctyl-2,5′:2′,5′′:2′′,2′′′:5′′′,2′′′′:5′′′′,2′′′′′:5′′′′′,2′′′′′′-septithiophene (DCN7T), which is composed of seven thiophene rings substituted with two terminal electron-withdrawing dicyanovinyl-substituent end groups.

The chemical structure of DCN7T is shown in Fig. 1(a) and the synthesis of DCN7T was described elsewhere.[16]

The photovoltaic devices were made by using a common fabrication process. The active layer was prepared by spin coating the blends of DCN7T (8 mg ml^{-1}) and PCBM in chloroform in different weight ratios (wt/wt 1:x, x=0.6, 1.0, 1.4, and 1.8) onto a precleaned indium tin oxide (ITO) coated glass substrate, which was modified by spin-coated a thin layer of poly-(3,4-ethylenedioxythiophene):polystyrenesulfonate (PEDOT:PSS) (Baytron) as a hole extraction/electron blocking layer and then dried in nitrogen without further treatment. Finally, LiF and Al were thermally evaporated through a shadow mask on the active layer as a cathode. The schematic diagram of the solar cells based on DCN7T:PCBM is shown in Fig. 1(b), which has a structure of ITO (~17 Ω/sq) /PEDOT:PSS (40 nm)/DCN7T:PCBM
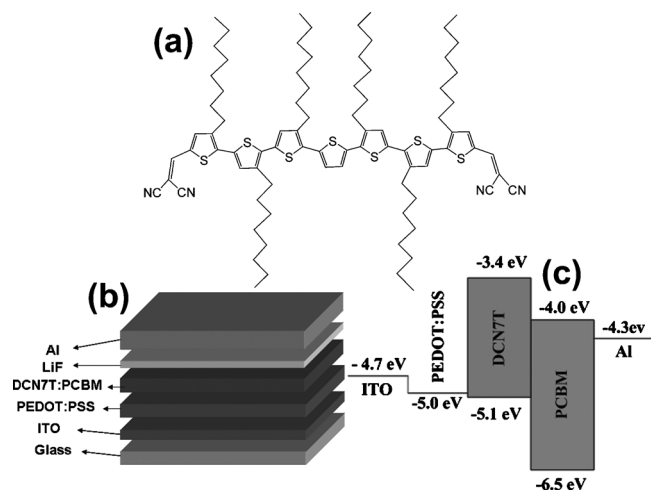

FIG. 1. (a) Chemical structure of DCN7T. (b) Schematic diagram of photovoltaic device based on DCN7T:PCBM. (c) Approximate HOMO/LUMO levels for DCN7T/PCBM based photovoltaic device.

a)Electronic mail: yinbin@mail.nankai.edu.cn.
b)Author to whom correspondence should be addressed. Electronic mail: sgyin@tjut.edu.cn. FAX: +86 (22) 6021-4010. Tel.: +86 (22) 6021-4019.
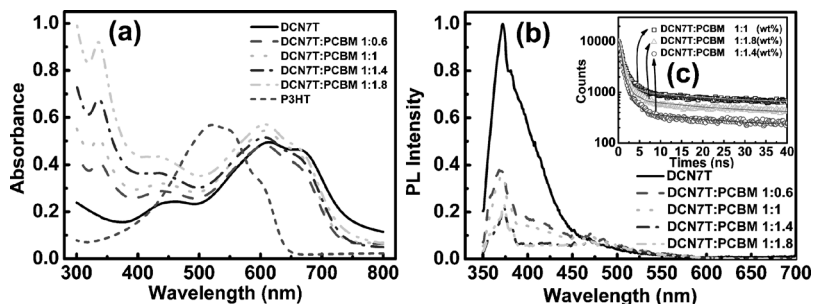
FIG. 2. (a) Absorption spectra of DCN7T, P3HT, and DCN7T:PCBM films in various weight ratios of 1:0.6, 1:1, 1:1.4, and 1:1.8. (b) PL spectra of DCN7T and DCN7T:PCBM in films with different ratios (wt/wt) excited with the wavelength of 250 nm. (c) Fluorescence decays of DCN7T:PCBM films with three different ratios as follows: 1:1 (hollow squares), 1:1.4 (hollow circles), and 1:1.8 (hollow triangles).

(110 nm)/LiF (1 nm)/Al (70 nm). The effective area of each cell is ~9 mm². The current density versus voltage (*J-V*) curves of the photovoltaic devices are recorded under simulated AM 1.5G with an illumination intensity of 100 mW/cm². A xenon lamp with a filter (broadpass GRB-3, Beijing Changtuo Scientific limited company) to simulate AM 1.5G conditions was used as the excitation source with a power of 100 mW/cm² white light illumination from the ITO side. Light source illumination intensity was measured using a calibrated broadband optical power meter (FZ-A, wavelength range 400–1000 nm, Photoelectric Instrument Co, Beijing Normal University, China).[17] The electrochemical band gap of DCN7T is about 1.7 eV as determined by cyclic voltammetry, while the optical band gap is about 1.68 eV,[16] indicating that the band gap of DCN7T is smaller than that of P3HT, which is approximately 2.0 eV.[18] The highest occupied molecular orbital (HOMO) and lowest unoccupied molecular orbital (LUMO) of DCN7T and PCBM, as well as other relevant energy levels are shown in Fig. 1(c).

The absorption spectra of the thin films of DCN7T, P3HT, and DCN7T/PCBM are presented in Fig. 2(a). The absorption spectrum of DCN7T film spreads from 400 to 800 nm, with a peak at 614 nm, indicating that DCN7T absorbs solar energy more effectively than P3HT, which absorbs photons in the range of 400–650 nm with a peak at 522 nm. In addition, it is important to note that a shoulder at 670 nm suggests a vibronic progression enforced by strong intermolecular interactions among the thiophene rings and the cyanovinyl-substituents in DCN7T molecule,[7,19] which is redshifted compare with that of P3HT (at 600 nm). It is obvious that the blend films of DCN7T/PCBM exhibit broader absorption spectra than that of the pure DCN7T due to the complementary absorption spectra between the DCN7T and PCBM, implying an effective solar photon harvest.

The photoluminescence (PL) spectra of DCN7T and DCN7T:PCBM with different weight ratios (1:0.6, 1:1, 1:1.4, and 1:1.8) are shown in Fig. 2(b). The films were prepared by spin-casting from chloroform solutions onto quartz

substrates. The pure DCN7T film displays a strong peak at 375 nm with excitation at 250 nm. The PL intensity of the film is remarkably reduced after doping with PCBM. The PL emission of DCN7T is more effectively quenched by increasing the weight of PCBM in the blends. Efficient PL quenching of the films with the weight ratios of 1:1.4 and 1:1.8 suggests that efficient exciton dissociation occurs at the interface between DCN7T and PCBM. Furthermore, the fluorescence decays of the DCN7T:PCBM films were measured by the JY FluoroLog 3 spectrophotometer using a 265 nm pulsed light-emitting diode, where the solid curves are biexponential fit to the experimental data and can be seen in Fig. 2(c). The fluorescence decay of DCN7T:PCBM blend (1:1.4) is significantly faster than those of the other two ratios, implying that in the film of 1:1.4 (wt/wt) the photogenerated excitons have a high possibility to diffuse to the interface between DCN7T and PCBM where they are dissociated to free charge carriers because the film has a better morphology.

The *J-V* curves of the photovoltaic devices based on DCN7T:PCBM, with two weight ratios of 1:0.6 and 1:1.4, in the dark and under illumination without annealing treatment are plotted in Fig. 3(a), which shows that under illumination of 100 mW/cm², the devices with a blended ratio of 1:1.4 (wt/wt) display obvious photoresponse. A PCE of 3.7%, open-circuit voltages (V_{oc}) of 0.88 V, fill factor (FF) of 0.34, and the short-circuit current densities (J_{sc}) of 12.4 mA cm⁻² are achieved. The *J-V* curves of the photovoltaic devices having different blend weight ratios (1:0.6, 1:1, 1:1.4, and 1:1.8 wt/wt) under AM 1.5G illumination with an intensity of 100 mW/cm² are shown in Fig. 3(b). Among the devices investigated so far, the PCE are 0.04%, 1.1%, 3.7%, and 3.2% for the devices with the ratios of 1:0.6, 1:1, 1:1.4, and 1:1.8, respectively. The efficiency of the solar cells increase with increasing PCBM weight and then decrease. The device with the ratio of 1:1.4 demonstrates the best performance. It is possible that in the case of small PCBM content, such as for 1:0.6 (wt/wt), the PCBM is too little to form an interpenetrating network morphology for exciton diffusing to and dissociating at the interface between two components. Be-
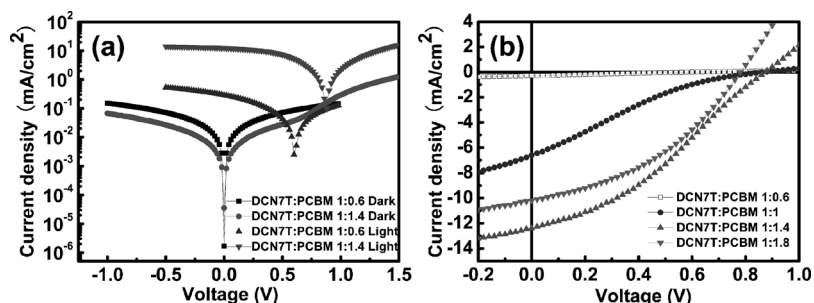

FIG. 3. (a) Logarithmic *J-V* characteristics of the photovoltaic devices based on different blends of DCN7T:PCBM 1:0.6, 1:1.4 (wt/wt) in dark and under AM 1.5G illumination (100 mW/cm²). (b) *J-V* curves of photovoltaic devices based on four blends of DCN7T:PCBM (1:0.6, 1:1, 1:1.4, and 1:1.8) (wt/wt) under AM 1.5G illumination.
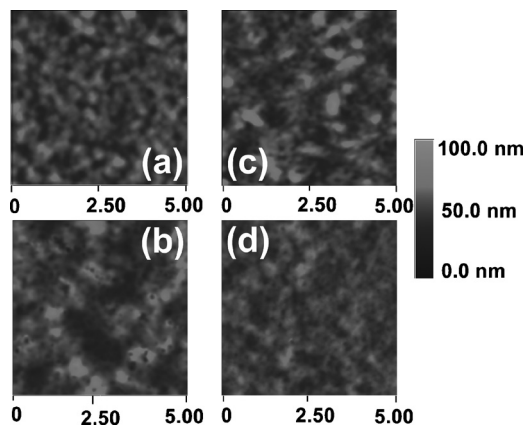
FIG. 4. Tapping mode AFM topography images (5×5 μm^2) of the four films cast from chloroform solutions of DCN7T:PCBM in various weight ratios as follows: (a) 1:0.6, (b) 1:1, (c) 1:1.4, and (d) 1:1.8.

sides that, with that ratio, PCBM is too little to form a continuous path for electron transport through the active layer to collection electrode. When the PCBM content increases in the blend, as in 1:1.4 (wt/wt), it is enough to produce an effective donor/acceptor interface for exciton dissociation and to form a percolation pathway for charge transport to the collection electrodes. The strong dependence of PCE on the blend ratios of the devices shows that the morphology influence on the performance of solar cells. As the PCBM content increased, as for 1:1.8 (wt/wt), aggregation may be occurring, which could deter exciton generation, separation and transport in the active layer. This is partly verified by the morphology variation among the blended films, as shown in topography images of atomic force microscopy (AFM) (Fig. 4). The topography image of pristine DCN7T film is smooth and the root-mean-square roughness is about 7.7 nm. After introducing PCBM into DCN7T, the three different donor/acceptor ratios show some phase segregation. The film with blend ratio of 1:1.4 exhibits a more continuous and rough morphology compared to the other two blend ratios and the corresponding device demonstrates the highest PCE.

The summary of the photovoltaic properties for these devices is given in Table I. Under AM 1.5G illumination, the $V_{oc} = 0.60 - 0.88$ V slightly depends on the blend ratios. The V_{oc} is based upon the difference in the LUMO level of the acceptor and the HOMO level of the donor because of the Fermi level pinning mechanism. In addition, the V_{oc} can be influenced by other factors such as, the ratios of the donor and the acceptor, processing conditions, etc.[20,21] The maximum V_{oc} of the devices based on DCN7T/PCBM is ~ 1.1 V, governed by the HOMO of DCN7T (5.1 eV) and the LUMO of PCBM (4.0 eV). The slightly lower V_{oc} of the devices may be caused by the loss of the carriers collected at the electrodes. In contrast, the dependence of J_{sc} on the weight ratios

of the two components is pronounced. For example, the J_{sc} increases from 0.29 to 12.4 mA cm^{-2}, when the blend ratio changes from 1:0.6 to 1:1.4, resulting in more than one order of magnitude improvement.

In conclusion, solution processed BHJ solar cells based on an oligothiophene derivative DCN7T was investigated. The oligothiophene derivative having two terminal electron-withdrawing groups exhibits an intermolecular donor-acceptor structure, which increases the absorption in the visible range.[22] The BHJ solar cell with DCN7T and PCBM at the ratio of 1:1.4 exhibits a PCE as high as 3.7% under AM 1.5G illumination with an intensity of 100 mW/cm^2 in air, which is among the highest efficiency to date for solution processed small molecule BHJ solar cells. The PCE of the BHJ solar cells can be further improved by tuning the molecular system and optimizing the device fabrication, however the FF of these devices are still low.

TABLE I. The V_{oc}, J_{sc}, FF, and PCE of the photovoltaic devices with different blends.

Ratios of the blends (wt/wt)	V_{oc} (V)	J_{sc} (mA cm^{-2})	FF	PCE (%)
DCN7T:PCBM (1:0.6)	0.60	0.29	0.23	0.04
DCN7T:PCBM (1:1)	0.88	6.6	0.19	1.1
DCN7T:PCBM (1:1.4)	0.88	12.4	0.34	3.7
DCN7T:PCBM (1:1.8)	0.78	10.2	0.40	3.2

[1]A. C. Mayer, S. R. Scully, B. E. Hardin, M. W. Rowell, and M. D. McGehee, Mater. Today **10**, 28 (2007).
[2]R. Po, M. Maggini, and N. Camaioni, J. Phys. Chem. C **114**, 695 (2010).
[3]G. Dennler, M. C. Scharber, T. Ameri, P. Denk, K. Forberich, C. Waldauf, and C. J. Brabec, Adv. Mater. (Weinheim, Ger.) **20**, 579 (2008).
[4]J. Y. Kim, K. Lee, N. E. Coates, D. Moses, T. Q. Nguyen, M. Dante, and A. J. Heeger, Science **317**, 222 (2007).
[5]W. W. Li, C. Du, F. H. Li, Y. Zhou, M. Fahlman, Z. S. Bo, and F. L. Zhang, Chem. Mater. **21**, 5327 (2009).
[6]Y. Yang, J. Zhang, Y. Zhou, G. J. Zhao, C. He, Y. F. Li, M. Andersson, O. Inganas, and F. L. Zhang, J. Phys. Chem. C **114**, 3701 (2010).
[7]C. Uhrich, R. Schueppel, A. Petrich, M. Pfeiffer, K. Leo, E. Brier, P. Kilickiran, and P. Baeuerle, Adv. Funct. Mater. **17**, 2991 (2007).
[8]F. Silvestri, M. D. Irwin, L. Beverina, A. Facchetti, G. A. Pagani, and T. J. Marks, J. Am. Chem. Soc. **130**, 17640 (2008).
[9]R. de Bettignies, Y. Nicolas, P. Blanchard, E. Levillain, J. M. Nunzi, and J. Roncali, Adv. Mater. (Weinheim, Ger.) **15**, 1939 (2003).
[10]A. B. Tamayo, X. D. Dang, B. Walker, J. Seo, T. Kent, and T. Q. Nguyen, Appl. Phys. Lett. **94**, 103301 (2009).
[11]A. B. Tamayo, B. Walker, and T. Q. Nguyen, J. Phys. Chem. C **112**, 11545 (2008).
[12]P. F. Xia, X. J. Feng, J. P. Lu, S. W. Tsang, R. Movileanu, Y. Tao, and M. S. Wong, Adv. Mater. (Weinheim, Ger.) **20**, 4810 (2008).
[13]G. D. Wei, S. Y. Wang, K. Renshaw, M. E. Thompson, and S. R. Forrest, ACS Nano **4**, 1927 (2010).
[14]J. G. Mei, K. R. Graham, R. Stalder, and J. R. Reynolds, Org. Lett. **12**, 660 (2010).
[15]B. Walker, A. B. Tomayo, X. D. Dang, P. Zalar, J. H. Seo, A. Garcia, M. Tantiwiwat, and T. Q. Nguyen, Adv. Funct. Mater. **19**, 3063 (2009).
[16]Y. S. Liu, J. Y. Zhou, X. J. Wan, and Y. S. Chen, Tetrahedron **65**, 5209 (2009).
[17]Q. Liu, Z. F. Liu, X. Y. Zhang, L. Y. Yang, N. Zhang, G. L. Pan, S. G. Yin, Y. S. Chen, and J. Wei, Adv. Funct. Mater. **19**, 894 (2009).
[18]K. Colladet, S. Fourier, T. J. Cleij, L. Lutsen, J. Gelan, D. Vanderzande, L. H. Nguyen, H. Neugebauer, S. Sariciftci, A. Aguirre, G. Janssen, and E. Goovaerts, Macromolecules **40**, 65 (2007).
[19]M. Turbiez, P. Frere, M. Allain, C. Videlot, J. Ackermann, and J. Roncali, Chem.-Eur. J. **11**, 3742 (2005).
[20]C. J. Brabec, A. Cravino, D. Meissner, N. S. Sariciftci, T. Fromherz, M. T. Rispens, L. Sanchez, and J. C. Hummelen, Adv. Funct. Mater. **11**, 374 (2001).
[21]Q. Liu, Z. F. Liu, X. Y. Zhang, N. Zhang, L. Y. Yang, S. G. Yin, and Y. S. Chen, Appl. Phys. Lett. **92**, 223303 (2008).
[22]S. Roquet, A. Cravino, P. Leriche, O. Aleveque, P. Frere, and J. Roncali, J. Am. Chem. Soc. **128**, 3459 (2006).